Title
Sodium Channel Activation Gating Is Affected by Substitutions of Voltage Sensor Positive Charges in All Four Domains

Journal
The Journal of General Physiology, 110(4)

ISSN
0022-1295

Authors
Kontis, Kris J
Rounaghi, Amir
Goldin, Alan L

Publication Date
1997-10-01

DOI
10.1085/jgp.110.4.391

Kontis, K.J., A. Rounaghi, and A.L. Goldin.
The Journal of General Physiology. Volume 110, No. 4, October 1997.

Page 400.

Table IV referred to previous data from Chen et al. (1996) concerning mutations in domain IV of the sodium channel. However, the numbering system for mutations in domain IV used by Chen et al. (1996) differed from that used in this paper. Therefore, two mutants were labeled incorrectly. Mutant 4R1Q should have been termed 4R0Q, and mutant 4R3Q should have been termed 4R2Q. The corrected table is reprinted below.

TABLE IV

Summary of Charge-neutralizing Mutation Effects on Activation

Mutant	$v_{1/2}$ shift*	z_m change (e_0)*
	mV	
1R1Q‡	+3.3	−0.6
1R1Q§	−2.0	0.0
1R2Q	−1.0	+0.4
1R2Q§	−8.0	−1.8‖
1R3Q‡	+4.7π	−1.7π
1R3Q§	+12.0	−1.5‖
1K4Q	+18.5π	−1.2π
1K4Q§	+19.0	−0.9‖
2R1Q‡	+13.3π	−1.2π
2R2Q	+4.4π	−1.1π
2R3Q‡	+0.4π	−1.6π
2K4Q	+14.9π	−0.7
2K5Q§	+10.0	0.0
3K1Q‡	−10.4π	−0.5
3R2Q	−0.3	+0.4
3R3Q‡	+5.9π	−2.1π
3R4Q	−18.1π	+0.3
4R0Q‡	+2.3	−1.6π
4R2Q	+3.6π	−0.5
4R2Q‡	+8.6π	−1.6π
4R4Q	+0.4	+0.9

*$v_{1/2}$ and z_m are the half-maximal voltage and gating valence of activation. Data from Stühmer et al. (1989) did not include an assessment of statistical significance. ‡Data from Chen et al. (1996). §Data from Stühmer et al. (1989). ‖The values for z_m from Stühmer et al. (1989) were multiplied by three for comparison because those values were based on three identical gating charges (m^3). πValues statistically significant, with a probability <0.05 resulting from random variation.

Sodium Channel Activation Gating Is Affected by Substitutions of Voltage Sensor Positive Charges in All Four Domains

Kris J. Kontis, Amir Rounaghi, and Alan L. Goldin

From the Department of Microbiology and Molecular Genetics, University of California, Irvine, Irvine, California 92697-4025

ABSTRACT The role of the voltage sensor positive charges in the activation and deactivation gating of the rat brain IIA sodium channel was investigated by mutating the second and fourth conserved positive charges in the S4 segments of all four homologous domains. Both charge-neutralizing (by glutamine substitution) and -conserving mutations were constructed in a cDNA encoding the sodium channel α subunit that had fast inactivation removed by the incorporation of the IFMQ3 mutation in the III–IV linker (West, J.W., D.E. Patton, T. Scheuer, Y. Wang, A.L. Goldin, and W.A. Catterall. 1992. *Proc. Natl. Acad. Sci. USA*. 89:10910–10914.). A total of 16 single and 2 double mutants were constructed and analyzed with respect to voltage dependence and kinetics of activation and deactivation. The most significant effects were observed with substitutions of the fourth positive charge in each domain. Neutralization of the fourth positive charge in domain I or II produced the largest shifts in the voltage dependence of activation, both in the positive direction. This change was accompanied by positive shifts in the voltage dependence of activation and deactivation kinetics. Combining the two mutations resulted in an even larger positive shift in half-maximal activation and a significantly reduced gating valence, together with larger positive shifts in the voltage dependence of activation and deactivation kinetics. In contrast, neutralization of the fourth positive charge in domain III caused a negative shift in the voltage of half-maximal activation, while the charge-conserving mutation resulted in a positive shift. Neutralization of the fourth charge in domain IV did not shift the half-maximal voltage of activation, but the conservative substitution produced a positive shift. These data support the idea that both charge and structure are determinants of function in S4 voltage sensors. Overall, the data supports a working model in which all four S4 segments contribute to voltage-dependent activation of the sodium channel.

KEY WORDS: voltage sensor • deactivation • expression • mutagenesis

INTRODUCTION

The voltage-dependent activation of sodium channels is essential for the generation of the upstroke phase of the action potential in most excitable cells. In brain neurons, the sodium channel consists of an α and two accessory β subunits (Catterall, 1984), but it has been shown in heterologous expression systems that the α subunit alone is sufficient to produce functional sodium channels (Noda et al., 1986; Goldin et al., 1986). The amino acid sequence of the sodium channel α subunit has been determined. The channel consists of four homologous domains that are 50–70% identical at the amino acid level (Noda and Numa, 1987). Hydropathy analysis suggests that each domain is made up of six transmembrane segments, termed S1–S6, and two segments that extend partially through the membrane to form part of the pore (Durell and Guy, 1992). Voltage-gated calcium and potassium channels have similar structural features, with the exception that potassium channel genes encode a single homologous domain that is functional as a tetramer (Jan and Jan, 1989). A key feature that these voltage-gated channels share is the amphiphilic S4 segment, containing multiple repeats of a motif consisting of a positively charged residue followed by two hydrophobic ones. The S4 positive charges are the only positive residues predicted to be within the membrane potential. Therefore, the S4 segments are believed to be the voltage-sensing apparatus of the channel that was originally proposed by Hodgkin and Huxley (1952).

The voltage sensor hypothesis predicts that positive charges within the sodium channel S4 segments, and possibly other residues, determine the voltage-dependent properties of the channel. The involvement of S4 positive charges in voltage-dependent gating of sodium channels was first shown by Stühmer et al. (1989). They found that neutralization of S4 positive charges in domains I and II of the rat brain II sodium channel shifted the voltage dependence of activation and decreased the apparent gating valence, consistent with the hypothesis that the charged residues serve as voltage sensors. However, analysis of the role of the S4 residues in potassium channels has clearly demonstrated

Dr. Kontis' present address is Hycor Biomedical Inc., Garden Grove, CA 92841.

Address correspondence to Dr. Alan L. Goldin, Department of Microbiology and Molecular Genetics, University of California, Irvine, Irvine, CA 92697-4025. Fax: 714-824-8598; E-mail: AGoldin@uci.edu

that there is not a direct correlation between the individual charges and the gating valence, although there is a relationship between the number of positive charges and the gating charge (Papazian et al., 1991; Liman et al., 1991; Logothetis et al., 1992, 1993; Tytgat et al., 1993). In addition, substitutions of hydrophobic residues in either sodium or potassium channels can have even larger effects on gating (Auld et al., 1990; Lopez et al., 1991; McCormack et al., 1993; Fleig et al., 1994). The best estimates for the size of the gating charges in the *Shaker* potassium channel (Schoppa et al., 1992) and the skeletal muscle sodium channel (Hirschberg et al., 1995) are that ~12 charges must move across the field during activation, which is easier to explain if all four S4 segments are involved in gating (Hirschberg et al., 1995). Recent experiments have shown that the domain IV S4 segment of the sodium channel (Yang and Horn, 1995; Yang et al., 1996) and the S4 segment of the *Shaker* potassium channel (Mannuzzu et al., 1996; Larsson et al., 1996) actually move during gating, and that some of the charged residues directly contribute to the gating charge (Perozo et al., 1994; Aggarwal and MacKinnon, 1996).

Most of the studies examining the role of the S4 charges have been carried out on the voltage-gated potassium channel, which functionally contains four identical S4 segments. It is probable that sequence divergence of the four domains in the sodium channel resulted in differential roles of each of the S4 segments. Such specialization would be consistent with the original formulation of Hodgkin and Huxley (1952), in which potassium channels contain four identical gates, whereas sodium channels contain three activation gates and one inactivation gate. It has previously been proposed that the S4 region of domain IV plays a unique role in coupling sodium channel activation to inactivation (Chahine et al., 1994; O'Leary et al., 1995). More recently, Chen et al. (1996) examined the importance of the S4 charges in the all four domains of the human heart sodium channel, confirming that the S4 region of domain IV is uniquely involved in sodium channel inactivation.

To investigate the role played by the four S4 segments in the voltage dependence of activation and deactivation, we constructed charge-neutralizing and -conserving substitutions of the second and fourth positive charges in the S4 segment of each domain of the rat brain IIA (RBIIA)[1] channel. We show that the positively charged residues in all four S4 segments contribute unequally to the voltage-dependent properties of the channel, consistent with the hypothesis that the different domains have specialized roles in gating.

[1]*Abbreviation used in this paper:* RBIIA, rat brain IIA.

MATERIALS AND METHODS

Sodium Channel Mutations and In Vitro Transcription

The parent construct used in all experiments was the cDNA encoding the α subunit of the RBIIA voltage-gated sodium channel that had the IFMQ3 mutation in the III–IV linker, which removes fast inactivation (West et al., 1992). This mutation was included because activation is not complete before inactivation begins at many voltages (Aldrich et al., 1983). Therefore, if inactivation is intact, the measured peak macroscopic current is less than the theoretical peak current as determined by activation alone. All of the mutations were made by site-directed mutagenesis using M13 subclones of the RBIIA channel, as previously described (Kontis and Goldin, 1993). The mutated fragments were ligated into the full length cDNA in a plasmid vector containing a T7 RNA polymerase promoter and *Xenopus* β globin 5′ and 3′ untranslated sequences. Capped, full length transcripts were generated in vitro using a T7 RNA transcription kit (Ambion Inc., Austin, TX), purified by phenol-chloroform extraction and ethanol precipitation, and dissolved in 10 mM Tris-HCl, pH 7.0, at ~1 μg/μl. Sodium channel β_1 subunit RNA was prepared by in vitro transcription from a plasmid containing the cDNA flanked by β globin sequences.

Expression of Channels in Xenopus Oocytes

Oocytes were removed from *Xenopus laevis* females and treated for 90–120 min with 2 mg/ml collagenase in OR-2 buffer (82.5 mM NaCl, 2 mM KCl, 1 mM $MgCl_2$, 5 mM HEPES, pH 7.5) to disperse the follicle cells. The oocytes were washed in the same buffer to remove residual collagenase, and then washed in ND96 (96 mM NaCl, 2 mM KCl, 1.8 mM $CaCl_2$, 1 mM $MgCl_2$, 5 mM HEPES, pH 7.5). The activation of sodium channels expressed in oocytes is very slow at negative potentials in the absence of the β_1 subunit, and does not reach complete saturation at potentials near the threshold of activation (Patton et al., 1994). To facilitate measurement of peak currents and activation kinetics over a wide voltage range, oocytes were co-injected with RNA encoding sodium channel α and β_1 subunits at an approximate molar ratio of $1\alpha:10\beta_1$. The dilution of α subunit RNA was determined empirically to achieve current amplitudes in the range of 0.5–5 μA. An excess of β_1 RNA was used in these experiments to assure that functional differences could not be attributed to limiting amounts of this subunit. The oocytes were injected in the center of the vegetal pole. Injected oocytes were incubated in ND96 containing 550 mg/liter sodium pyruvate, 0.5 mM theophylline, and 50 μg/ml gentamicin for 2 d at 20°C before electrophysiological recording.

Electrophysiological Recording

Voltage clamping of *Xenopus* oocytes was performed using the DAGAN CA-1 high performance oocyte clamp, DigiData 1200 Interface (DAGAN Corp., Minneapolis, MN) and pCLAMP software (version 6.0.3; Axon Instruments, Inc., Burlingame, CA). Oocytes were perforated with a 25-gauge needle in the center of the vegetal pole and were mounted on the voltage clamp stage fitted with a perfusion cannula connected to a syringe pump filled with internal solution. The internal solution was (mM): 88 K^+, 10 EGTA-CsOH, 10 HEPES-CsOH, and 10 Na^+, pH 7.5. The external solution consisted of (mM): 120 Na^+-methyl ethane sulfonate (MES), 10 HEPES-CsOH, 1.8 Ca^{++}-MES, pH 7.5. Care was taken to exclude chloride ions in making these solutions to avoid potential interference from native oocyte chloride channel currents. Agarose bridges coupling the headstage to the bath were filled with 0.5% low melting point agarose in 1 M NaOH-MES

(pH 7.5) and were fitted with 100-μm platinum wires to improve frequency response. The headstage manifold wells were filled with 1 M NaCl. The temperature in these experiments was regulated at 15°C by a Peltier device coupled to a feedback controller (HCC-100A; DAGAN Corp.). Voltage was monitored through a 0.2–0.5 MΩ microelectrode filled with 3 M KCl, which was inserted through the animal pole of the oocyte.

Oocytes were maintained at 15°C and clamped at −100 mV for at least 5 min to allow temperature equilibration and full recovery from inactivation. Current–voltage data were acquired using a sampling rate of 50 kHz with a filter frequency of 10 kHz. Depolarizations from a holding potential of −100 mV ranged from −90 to +55 mV in 5-mV steps, and lasted 57.5 ms. In the case of some mutants, the voltage range of depolarizations was modified to compensate for shifts in $v_{1/2}$. Instantaneous tail currents were acquired with the same sampling and filter frequencies using a two-pulse protocol. The first step was a depolarization to +20 mV for 1–3 ms to achieve maximal activation. For mutants that had large positive shifts in activation, this prepulse was to +60 mV. The second step was a 33.7-ms depolarization ranging from −90 to +55 mV in 5-mV steps. All data were acquired using P/4 subtraction and capacitance compensation. The series resistance ranged from 1 to 1.5 kΩ.

Data Analysis

Electrophysiological data were analyzed using pCLAMP software. Maximum inward tail currents were measured after repolarization to −100 mV for each current–voltage data record. Nonlinear curve fitting was performed using Sigmaplot (version 4.0; Jandel Scientific, San Rafael, CA), which uses the Marquardt-Levenberg algorithm for nonlinear regression. The fraction of activated channels was calculated by measuring the peak inward current after repolarization to −100 mV from depolarizations ranging from −90 to +55 mV, and normalizing the values to the maximum inward current. Normalized current–voltage relationships were fitted with a two-state Boltzmann function,

$$I/I_{max} = 1/\{1 + \exp[-F/RT \cdot z_m \cdot (v - v_{1/2})]\}, \quad (1)$$

where I/I_{max} is the normalized current after repolarization, $v_{1/2}$ is the half-maximal voltage of activation, and z_m is the apparent gating valence.

Activation kinetics were measured by fitting the rising phase of current traces during step depolarizations to a single exponential equation,

$$I = A \cdot \exp[-(t-k)/\tau_m] + C, \quad (2)$$

where I is the current, A is the initial amplitude, $(t - k)$ is the interval over which the fit is applied, τ_m is the time constant, and C is the baseline. The voltage dependence of the activation kinetics was analyzed over a voltage range of −30 to +30 mV by fitting the data to an equation describing a single voltage-dependent exponential:

$$\tau_m = \tau_0 \cdot \exp[-k \cdot (FV/RT)] + \tau_{min}, \quad (3)$$

where τ_0 is the time constant at 0 mV membrane potential (corrected by subtracting the baseline, τ_{min}), k is the constant of voltage dependence, and τ_{min} is the lower limit of the activation time constant.

Deactivation kinetics were measured by fitting the instantaneous tail currents to the single exponential equation,

$$I = A \cdot \exp[-(t-k)/\tau_d] + C, \quad (4)$$

where τ_d is the time constant for deactivation and I, A, $(t - k)$, and C have the same meanings as in Eq. 2. The voltage dependence of the deactivation kinetics was measured by fitting the data to a voltage-dependent single exponential equation,

$$\tau_d = \tau_{-50} \cdot \exp[k \cdot (v + 50) \cdot F/RT] + \tau_{min}, \quad (5)$$

where τ_{-50} is the deactivation time constant at a membrane potential of −50 mV (corrected by subtracting the baseline, τ_{min}), k is the constant of the voltage-dependent variation of deactivation kinetics, and τ_{min} is the lower limit of the deactivation time constant. The average and standard deviations for each voltage-dependent parameter were determined by individually fitting the data. Statistical significance was evaluated using Student's unpaired t test.

RESULTS

Voltage Dependence of Activation Is Shifted by Substitution of Some, but Not All, Positive Charges in Each S4 Domain

The voltage-gated sodium channel consists of four homologous domains that each contain six segments (S1–S6) that completely traverse the cell membrane (Guy and Seetharamulu, 1986). The S4 segments are highly amphiphilic, each having from four to eight positively charged residues. Our working model of the sodium channel predicts that all four domains participate in

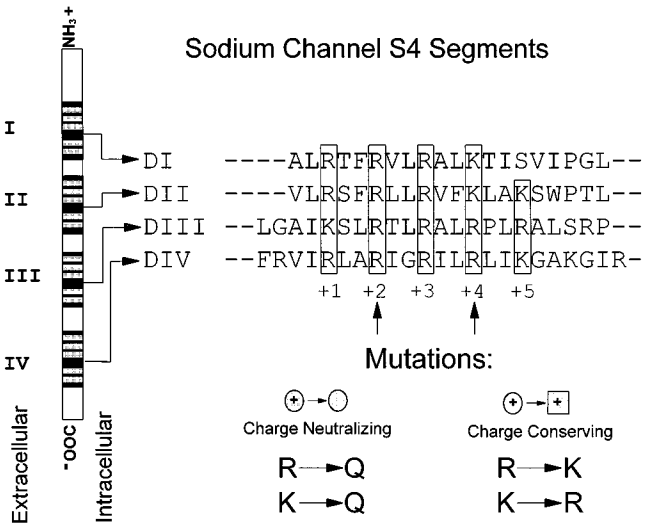

FIGURE 1. Amino acid sequence alignment of the S4 segments of the RBIIA sodium channel. The sodium channel is diagrammed on the left, depicting the four homologous domains (*I–IV*), each consisting of six transmembrane segments. The amino acid sequences of the four S4 regions are shown on the right. Site-directed mutagenesis was used to substitute the second and fourth conserved positive charges in each domain. Both charge-neutralizing, in which glutamine was substituted, and charge-conserving mutations were constructed. For simplicity, residues are named by the domain and position in the S4 segment, and correspond to the actual amino acid positions as follows: 1R2 = R220, 1K4 = K226, 2R2 = R853, 2K4 = K859, 3R2 = R1306, 3R4 = R1312, 4R2 = R1632, and 4R4 = R1638. The names of the mutations include the amino acid that was substituted. For example 1R2Q is a mutation in domain I S4 substituting the second positive charge arginine (R220) with glutamine (Q).

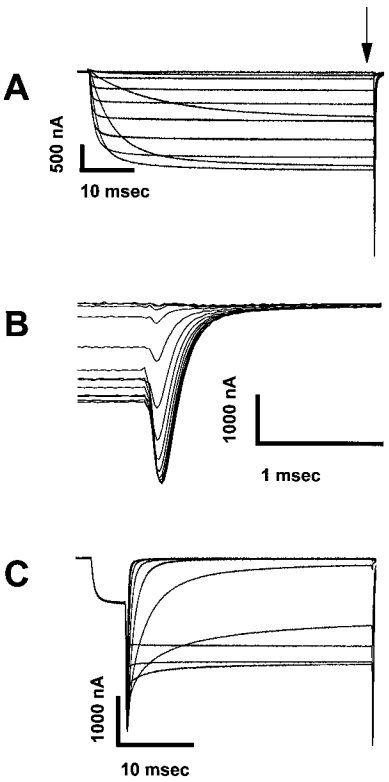

FIGURE 2. Representative current traces showing the activation and deactivation kinetics of the RBIIA channel containing the IFMQ3 mutation. *Xenopus* oocytes were co-injected with in vitro transcribed RNA encoding the sodium channel α and β_1 subunits. After a 2-d incubation at 20°C, data were recorded using the cut-open oocyte voltage clamp method as described in MATERIALS AND METHODS. (*A*) Current traces recorded during 57.5-ms depolarizations ranging from −50 to +50 mV. The IFMQ3 mutation removes fast inactivation, and all of the S4 mutations were made in this background. The tail currents occurring after repolarization are indicated by the vertical arrow in *A* and are shown in greater detail in *B*. (*C*) Instantaneous tail currents from the same oocyte were recorded after activation of the channels with a prepulse to +20 mV for 2 ms, followed by 75-ms steps to voltages ranging from −90 to 0 mV in 10-mV increments.

the voltage-dependent conformational changes that are manifested in the electrophysiological behavior of the channel. To examine the role of the voltage sensors of the sodium channel in activation gating, point mutations were made in the S4 segment of each domain. The sequences of the S4 segments are aligned in Fig. 1 to show the repeated motif of a positively charged residue followed by two hydrophobic residues. The numbering shown labels the positive charges starting from the extracellular end of each segment toward the intracellular end, so that the first positive charge in domain I is called 1R1. In this labeling system, substitution of the second positive charge of the domain I S4 segment with a glutamine is denoted as 1R2Q. Single mutants were constructed in which charge neutralizing (glutamine) and charge conserving (arginine or lysine) substitutions were made for the second and fourth residues of each S4 segment. Two double mutants were also constructed, one that combines neutralizations of the fourth positive charges in domains I and II (1K4Q and 2K4Q), and the other combining neutralizations of the fourth positive charges in domains III and IV (3R4Q and 4R4Q).

To measure peak macroscopic currents without interference from inactivation, all mutations were made in the RBIIA sodium channel containing the IFMQ3 mutation, which removes fast inactivation (West et al., 1992). Fig. 2 *A* shows representative currents from IFMQ3, demonstrating that the channels activate and remain open for the duration of the 50-ms depolarization. The tail currents visible upon repolarization (Fig. 2 *A*, *arrow*) are shown in greater detail in Fig. 2 *B*, and reflect the peak conductance upon repolarization to −100 mV. The traces in Fig. 2 *C* represent tail currents elicited after fully activating all channels with a 2–3-ms depolarization to +20 mV, followed by 75-ms steps to voltages ranging from −90 to +55 mV. The time course of the current decay during these voltage steps reflects sodium channel deactivation.

The voltage dependence of activation for IFMQ3 and all of the mutant channels is shown in Fig. 3, which depicts the normalized peak tail currents (as determined in Fig. 2 *B*) plotted against the depolarization potential. Parameters of the Boltzmann fits to the data are shown in Table I. The gating valences were determined from the slopes of the Boltzmann equations. Although most of the mutations resulted in statistically significant shifts in the $v_{1/2}$ for activation, only a few caused pronounced changes. The largest shifts were observed when the fourth positive charge was neutralized. Neutralization of the fourth charge in domain I (1K4Q) or II (2K4Q) resulted in a significant positive shift in $v_{1/2}$, and the combination of the two substitutions (1K4Q:2K4Q) resulted in a positive shift that was greater than the sum of the two individual changes. The substitution in domain I also significantly decreased the gating valence, and the double substitution resulted in an even greater reduction in valence.

In contrast, neutralization of the fourth positive charge in domain III (3R4Q) resulted in a negative shift in $v_{1/2}$. However, the charge-conserving substitution of the same residue (3R4K) resulted in a positive shift, emphasizing the importance of both charge and structure at this position. No significant shift was observed for neutralization of the fourth charge in domain IV (4R4Q). In addition, none of the substitutions in either domain III or IV significantly affected the gating valence. Combining the two substitutions of the fourth charge in domains III and IV (3R4Q:4R4Q) resulted in a channel with properties similar to 3R4Q alone, supporting the idea that charges in the S4 segment of

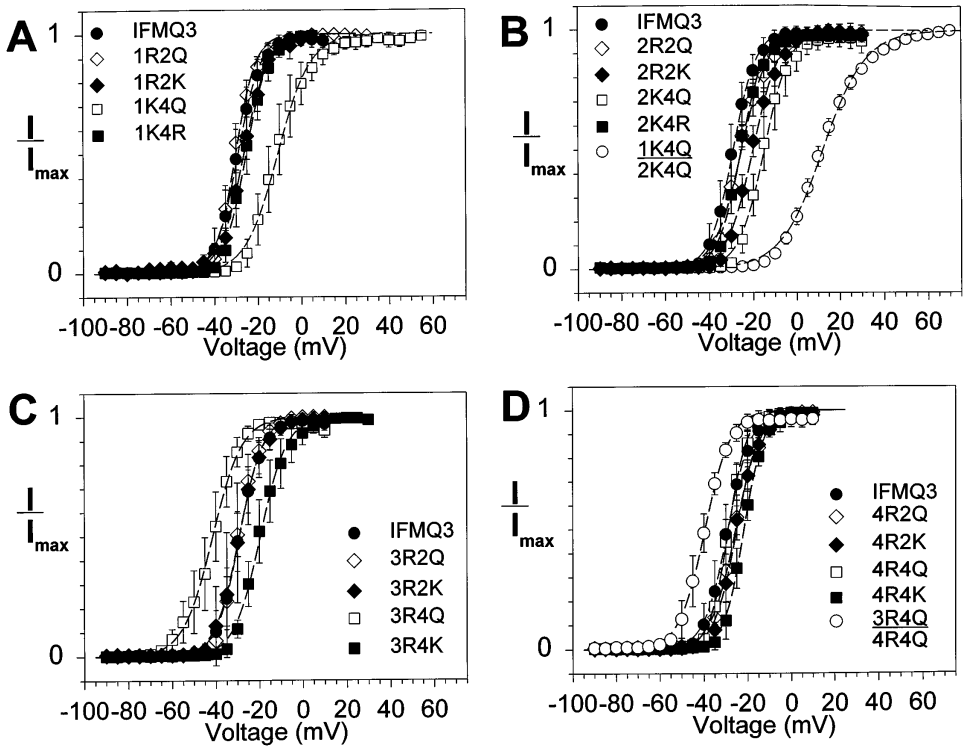

FIGURE 3. Effects of S4 mutations on the voltage dependence of activation. *Xenopus* oocytes were injected with RNA encoding the IFMQ3 channel or each of the S4 mutants, along with RNA encoding the β_1 subunit. Currents were recorded from a holding potential of −100 mV by depolarizations ranging from −90 to +55 mV, as described in MATERIALS AND METHODS. The fraction of sodium channels activated at each potential was determined, and is plotted as a function of voltage. Data are shown for the mutants in domains I (*A*), II (*B*), III (*C*), and IV (*D*). Data for the double mutants are shown in *B* and *D*. The data points represent the means of at least three determinations and the error bars show the standard deviations. The smooth lines are fits to a two-state Boltzmann function, as described in MATERIALS AND METHODS. The parameters of the fits are included in Table I.

domain IV are not as involved in voltage-dependent activation.

Mutations of Positive Charges in the S4 Voltage Sensors Can Affect the Voltage Dependence of Activation Kinetics

The voltage dependence of sodium channel activation is reflected in the behavior of activation kinetics over a defined voltage range. Fig. 4 shows the time constants obtained by fitting the current data obtained from IFMQ3 with a single exponential equation as described in MATERIALS AND METHODS. The value τ_{min} is the minimum approached as v becomes more positive and the constant k defines the voltage dependence. The value of k can be used to calculate the voltage step required for an e-fold change in τ_m for the condition when τ_{min} goes to zero, since the relevant issue is the effect of the charge, not the limiting τ_{min}. The term τ_0 represents the value of τ_m when there is no potential across the membrane after subtracting τ_{min}.

Data for all of the mutants were similarly analyzed, and the activation time constants are plotted on a log scale against step potential in Fig. 5, with the parameters of the fits shown in Table II. Differences in τ_0 between each of the mutants and IFMQ3 can be expressed as a shift along the voltage axis, assuming that there is no difference in *k* between the mutant and IFMQ3 channels. Although this assumption is not completely correct for most of the mutants, the values for *k* are similar enough between the mutants and IFMQ3 so

TABLE I

Parameters of the Voltage Dependence of Activation

Channel	$v_{1/2}$*	z_m (e_0)*	*n**
	mV		
IFMQ3	−29.1 ± 2.7	5.1 ± 1.1	10
1R2Q	−30.1 ± 1.6	5.5 ± 0.6	4
1R2K	−26.3 ± 1.7	4.6 ± 0.5	3
1K4Q	−10.6 ± 3.5‡	3.9 ± 0.6‡	7
1K4R	−25.3 ± 2.5‡	5.1 ± 0.3	7
2R2Q	−24.7 ± 1.5‡	4.0 ± 0.8‡	7
2R2K	−20.0 ± 1.8‡	4.2 ± 0.5	4
2K4Q	−14.2 ± 3.1‡	4.4 ± 0.9	5
2K4R	−25.3 ± 1.0‡	4.9 ± 1.3	5
3R2Q	−29.4 ± 1.9	5.5 ± 0.4	5
3R2K	−29.5 ± 5.2	5.5 ± 0.5‡	4
3R4Q	−47.2 ± 6.4‡	5.4 ± 1.6	5
3R4K	−19.3 ± 3.3‡	4.5 ± 0.9	8
4R2Q	−25.5 ± 1.7‡	4.6 ± 0.4	5
4R2K	−25.0 ± 1.7‡	5.1 ± 0.4	3
4R4Q	−28.7 ± 1.6	6.0 ± 0.8	7
4R4K	−21.7 ± 1.5‡	5.7 ± 0.3	5
1K4Q:2K4Q	−12.2 ± 1.4‡	2.6 ± 0.2‡	7
3R4Q:4R4Q	−39.4 ± 1.7‡	4.5 ± 0.9	6

*$v_{1/2}$ and z_m are the half-maximal voltage and gating valence of activation as determined by least-squares fits of the data (*n* = number of separate determinations) to a two-state Boltzmann function as described in MATERIALS AND METHODS. ‡Values significantly different from IFMQ3, with a probability <0.05 resulting from random variation (based on Student's unpaired *t* test).

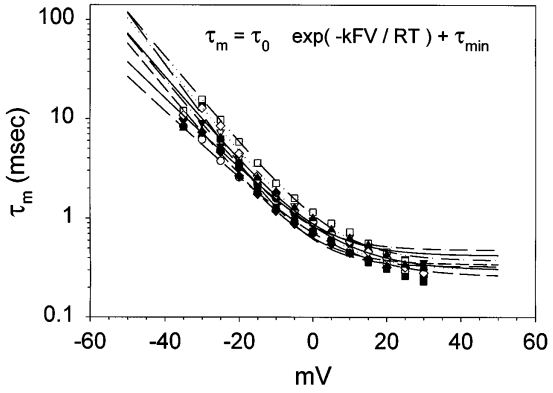

FIGURE 4. Determination of the voltage dependence of activation time constants in the IFMQ3 sodium channel. Sodium currents were recorded from oocytes expressing IFMQ3, as described in Fig. 3. The rising phase of the inward sodium currents was fit with a single exponential, as described in MATERIALS AND METHODS. Each data point represents a single determination and the smooth lines were generated by a least-squares fit to an equation (*inset*) describing the voltage-dependent variation of the activation time constant (τ_m). The parameters of the fits are shown in Table II.

that the calculated shifts are generally valid. That is, the value of the shift changed by <1.7 mV depending on whether the mutant or IFMQ3 value for k was used for all of the mutants except 1K4Q:2K4Q. For that double mutant, the calculated voltage shift was 24.7 mV if the mutant value for k was used.

As with the voltage dependence of activation, the most significant differences were observed for neutralizations of the fourth positive charges in domains I and II. Each of these neutralizations resulted in a positive voltage shift in τ_m, and the combination of the two resulted in a shift that was approximately the sum of the individual changes. Therefore, neutralization of either of these charges shifts the voltage dependence of both activation and activation kinetics in the positive direction.

Substitutions of the comparable charges in domains III and IV resulted in less dramatic effects on the kinetics of activation. The 3R4Q mutation resulted in a positive voltage shift in τ_m, in contrast to the negative shift in the voltage dependence of activation that was observed for the same mutant (Table I). The 4R4Q mutation caused a negative voltage shift in τ_m, and this mutant did not demonstrate any significant shift in the voltage dependence of activation. Combination of the two mutations (3R4Q:4R4Q) resulted in a channel with kinetics similar to those of IFMQ3, which is not surprising considering that each mutant shifts τ_m in the opposite direction.

Voltage Dependence of Deactivation Kinetics Is Altered by Some Positive Charge Mutations in the S4 Voltage Sensors

Upon returning to hyper-polarized membrane potentials, activated sodium channels rapidly deactivate. The rate of deactivation slows in a voltage-dependent manner as the membrane potential becomes more positive. Fig. 6 shows the time constants obtained by fitting the instantaneous tail currents obtained from IFMQ3 with

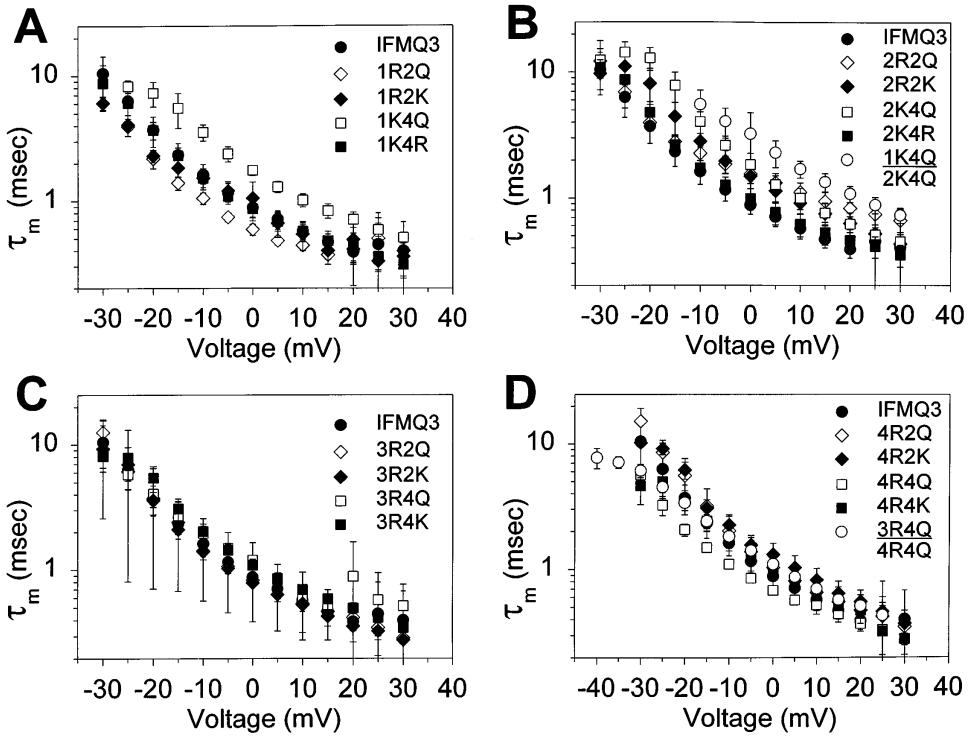

FIGURE 5. Effects of S4 mutations on the voltage dependence of activation time constants. Time constants of activation (τ_m) were determined for all of the mutants as described in Fig. 4. The values for potentials from −30 to +30 mV are shown for the mutants in domains I (*A*), II (*B*), III (*C*), and IV (*D*). Data for the double mutants are shown in *B* and *D*. The data points represent the means of at least three determinations and the error bars show the standard deviations. The parameters of the fits are shown in Table II.

TABLE II

Parameters of Activation Kinetics

Channel	τ_0*	v_{shift}‡	*k**	τ_{min}*	$v_{e\text{-fold change}}$§	*n**
	ms	*mV*		*ms*	*mV*	
IFMQ3	0.5 ± 0.1	n.a.‖	2.6 ± 0.3	0.4 ± 0.1	9.7	9
1R2Q	0.2 ± 0.0π	−9.9	3.1 ± 0.1π	0.4 ± 0.1	8.1	5
1R2K	0.4 ± 0.2	−2.2	2.4 ± 0.4	0.4 ± 0.1	10.2	5
1K4Q	1.1 ± 0.2π	8.6	2.3 ± 0.5	0.5 ± 0.1	10.8	6
1K4R	0.4 ± 0.1	−2.1	2.8 ± 0.3	0.4 ± 0.1	9.0	6
2R2Q	0.5 ± 0.1	1.4	2.4 ± 0.3	0.8 ± 0.2	10.5	5
2R2K	0.9 ± 0.2π	6.5	2.5 ± 0.3	0.5 ± 0.1	9.9	4
2K4Q	1.3 ± 0.4π	10.2	2.9 ± 0.3	0.5 ± 0.1	8.6	4
2K4R	0.4 ± 0.3	−2.1	3.0 ± 0.7	0.4 ± 0.2	8.4	5
3R2Q	0.4 ± 0.1	−1.9	2.7 ± 0.1	0.4 ± 0.3	9.3	5
3R2K	0.3 ± 0.1	−3.9	3.2 ± 0.4π	0.4 ± 0.1	7.8	4
3R4Q	0.8 ± 0.4π	5.5	2.0 ± 0.3π	0.5 ± 0.1	12.6	3
3R4K	0.6 ± 0.1	2.4	2.8 ± 0.3	0.4 ± 0.2	9.0	8
4R2Q	0.5 ± 0.2	1.2	3.0 ± 0.3π	0.4 ± 0.1	8.4	7
4R2K	0.3 ± 0.0	−2.7	2.6 ± 0.1	0.4 ± 0.1	9.5	3
4R4Q	0.2 ± 0.1π	−7.6	2.2 ± 0.3	0.3 ± 0.2	11.2	6
4R4K	0.4 ± 0.1	−1.5	2.1 ± 0.4	0.3 ± 0.1	11.6	7
1K4Q:2K4Q	2.4 ± 0.4π	16.2	1.7 ± 0.4π	0.3 ± 0.1	14.8	9
3R4Q:4R4Q	0.4 ± 0.1	−0.7	1.7 ± 0.2π	0.3 ± 0.1	14.7	8

*τ_0, τ_{min}, and *k* were determined by least-squares fits of the data (*n* = number of separate determinations) to a voltage-dependent single exponential as described in MATERIALS AND METHODS. ‡v_{shift} is the shift in voltage for the mutant τ_m compared with the IFMQ3 τ_m, calculated using the IFMQ3 value for *k*. §$v_{e\text{-fold change}}$ is the voltage required for an e-fold change in τ_m for the condition when $\tau_{min} << \tau_m$. ‖n.a., not applicable. πValues significantly different from IFMQ3, with a probability <0.05 resulting from random variation (based on Student's unpaired *t* test).

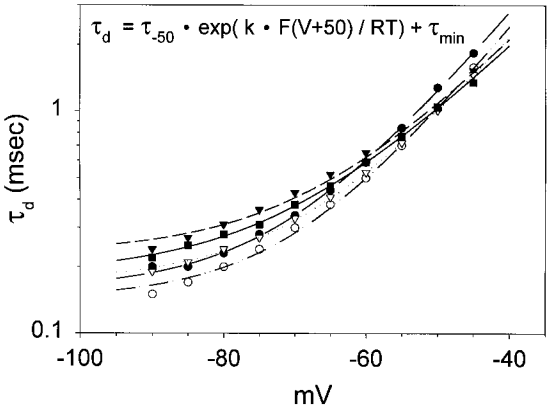

FIGURE 6. The voltage dependence of deactivation time constants can be fit by a single exponential. Sodium currents were recorded from oocytes expressing IFMQ3, as described in Fig. 3. Instantaneous tail currents were acquired by a depolarization to +20 mV for 1–3 ms, followed by a 33.7-ms depolarization ranging from –90 to –45 mV in 5-mV increments. The smooth lines represent the best fits to a voltage-dependent single exponential equation (*inset*). The parameters of the fits are shown in Table III.

a single exponential equation as described in MATERIALS AND METHODS. The term τ_{-50} is the time constant at a membrane potential of −50 mV after subtracting the baseline (τ_{min}), k is the exponential constant, and τ_{min} is the minimum time constant approached at increasingly negative potentials. As with activation, k can be used to calculate the voltage step required for an e-fold change in τ_d for the condition when τ_{min} goes to zero, and differences in τ_{-50} can be expressed as shifts along the voltage axis, with the same assumptions as described earlier for τ_m. The value of −50 mV was chosen arbitrarily because the τ_d values become extremely large and subject to greater error at 0 mV.

Data for all of the mutants were similarly analyzed, and the deactivation time constants are plotted on a log scale against step potential in Fig. 7. The values for τ_{-50}, voltage shift, k, and the voltage required for an e-fold change are shown in Table III. As was the case for the voltage dependence of activation and activation kinetics, neutralizations of the fourth positive charges had the most significant effects. Neutralization of the fourth charge in domains I or II resulted in a positive shift in τ_d, and neutralization of the fourth charge in domain III (3R4Q) resulted in a large negative shift. However, the charge-conserving mutation of the same residue (3R4K) caused a shift in the positive direction of comparable magnitude. The opposite effects of the charge-neutralizing and -conserving substitutions at this position are comparable with the results observed for the voltage dependence of activation. Substitution of the fourth charge in domain IV (4R4Q) resulted in no significant changes, as was the case for the parameters examined previously. However, combining the mutations in domains III and IV (3R4Q:4R4Q) resulted in the largest negative shift in deactivation kinetics.

DISCUSSION

This study examines the roles in activation gating of the four putative voltage sensors (S4 segments) in the sodium channel. Previous reports have demonstrated that the S4 regions in the sodium channel are involved in voltage-dependent gating (Stühmer et al., 1989; Chen et al., 1996), and our results are consistent with that interpretation. However, distinct differences were observed in the effects of comparable mutations in each of the four domains, suggesting that there is a significant extent of differentiation between the domains.

It is clear from previous results with sodium (Chen et al., 1996) and potassium (Papazian et al., 1991; Liman et al., 1991; Logothetis et al., 1992, 1993; Tytgat et al., 1993) channels that each of the charges in the S4 regions are not equally important for activation gating. In this study, elimination of charges at only five positions altered the $v_{1/2}$ for activation, and elimination of the charges at only two positions (1K4Q and 2R2Q) decreased the gating valence. The changes in gating va-

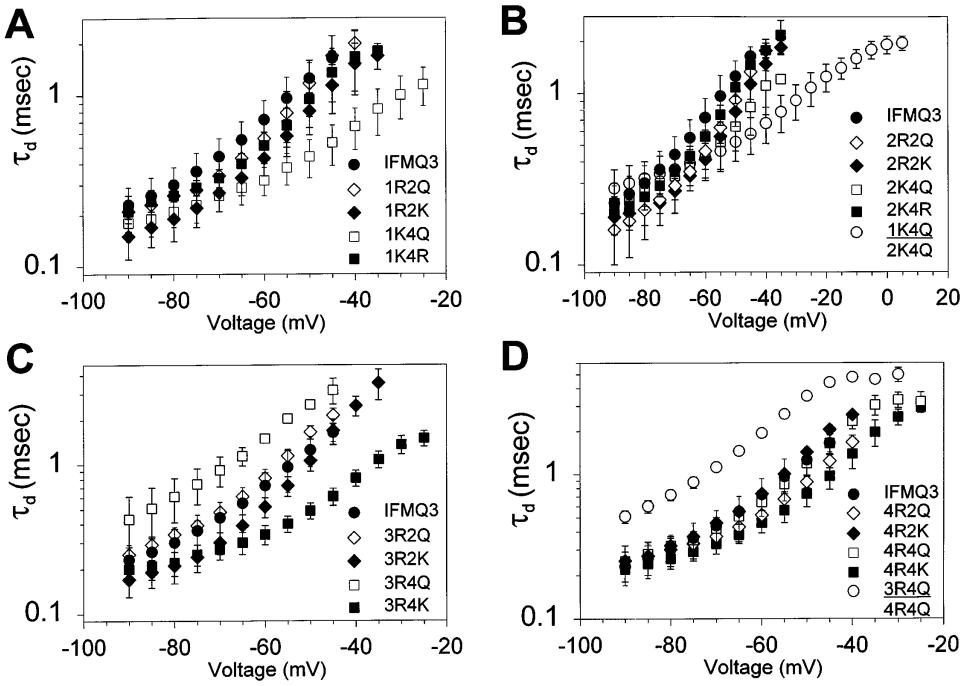

FIGURE 7. Effects of S4 mutations on the voltage dependence of deactivation time constants. Time constants of deactivation (τ_d) were determined for all of the mutants as described in Fig. 6. The values are shown for the mutants in domains I (*A*), II (*B*), III (*C*), and IV (*D*). Data for the double mutants are shown in *B* and *D*. The data points represent the means of at least three determinations and the error bars show the standard deviations. The parameters of the fits are shown in Table III.

lence must be considered approximations because these values were determined from the slope of the Boltzmann fits. Limiting slope analysis is a more accurate means of determining z_m, but it is necessary to measure current at extremely low probability of opening to approximate limiting slope (Sigworth, 1995). The measurement of such small currents was too unreliable in these experiments to provide informative data, although the general trends determined from limiting slope analysis were comparable with those determined from fits to the Boltzmann equation (data not shown).

Even if limiting slopes were used, it is not possible to accurately determine the extent to which any one charge functions as a voltage sensor for activation by this type of analysis, for a number of reasons. First, many of the mutations significantly shift the $v_{1/2}$ for activation, indicative of a change in the relative stabilities of the resting and activated states. This change could result from an interaction between the charged residue and an amino acid of the opposite charge elsewhere in the channel in one state, as has been shown to be the case for the *Shaker* potassium channel (Papazian et al., 1995). The net effect could be a reduction in the apparent gating valence. Second, the apparent overall gating event may be largely determined by one charge or domain that dominates the kinetic process. Therefore, the conductance–voltage curve will reflect the movement of that one gate, and neutralization of charges in other domains may have no effect on the measured gating valence. Finally, if any one charge represents just 1 of the 12 charges that move across the field during activation of the sodium channel (Hirschberg et al., 1995), then

TABLE III

Parameters of Deactivation Kinetics

Construct	τ_{-50}*	v_{shift}‡	*k**	τ_{min}*	$v_{e\text{-fold change}}$§	*n**
	ms	*mV*		*ms*	*mV*	
IFMQ3	0.9 ± 0.1	n.a.‖	2.1 ± 0.2	0.2 ± 0.1	11.7	5
1R2Q	1.0 ± 0.4	−0.9	2.5 ± 0.2π	0.2 ± 0.1	9.9	5
1R2K	0.7 ± 0.2	3.2	1.8 ± 0.1π	0.1 ± 0.1	13.6	4
1K4Q	0.3 ± 0.1π	12.3	1.3 ± 0.1π	0.1 ± 0.1	19.6	5
1K4R	0.8 ± 0.3	2.2	2.1 ± 0.3	0.2 ± 0.1	11.6	7
2R2Q	0.8 ± 0.1	1.7	2.0 ± 0.2	0.1 ± 0.1	12.7	8
2R2K	0.6 ± 0.1π	4.7	2.3 ± 0.2	0.2 ± 0.1	11.0	4
2K4Q	0.6 ± 0.2π	5.7	1.9 ± 0.2	0.2 ± 0.1	13.0	6
2K4R	0.9 ± 0.2	0.3	2.0 ± 0.3	0.2 ± 0.1	12.7	4
3R2Q	1.2 ± 0.4	−3.3	1.9 ± 0.1	0.2 ± 0.1	13.2	4
3R2K	1.1 ± 0.4	−2.4	2.3 ± 0.3	0.1 ± 0.1	10.8	4
3R4Q	2.4 ± 0.3π	−11.2	1.6 ± 0.3π	0.2 ± 0.2	15.5	3
3R4K	0.3 ± 0.1π	12.0	1.7 ± 0.2π	0.2 ± 0.1	15.0	4
4R2Q	0.7 ± 0.1π	3.8	2.0 ± 0.1	0.2 ± 0.1	12.5	5
4R2K	1.1 ± 0.5	−2.0	1.9 ± 0.3	0.2 ± 0.1	12.9	4
4R4Q	1.0 ± 0.2	−1.1	1.9 ± 0.1	0.2 ± 0.1	12.8	5
4R4K	0.6 ± 0.2π	5.3	1.8 ± 0.2π	0.2 ± 0.1	13.7	7
1K4Q:2K4Q	0.3 ± 0.1π	14.2	1.2 ± 0.1π	0.2 ± 0.1	21.6	9
3R4Q:4R4Q	3.0 ± 0.5π	−14.1	1.3 ± 0.2π	0.0 ± 0.2	19.0	6

*τ_{-50}, τ_{min}, and *k* were determined by least-squares fits of the data (*n* = number of separate determinations) to a voltage-dependent single exponential as described in MATERIALS AND METHODS. ‡v_{shift} is the shift in voltage for the mutant τ_d compared with the IFMQ3 τ_d, calculated using the IFMQ3 value for *k*. §$v_{e\text{-fold change}}$ is the voltage required for an e-fold change in τ_d for the condition when $\tau_{min} << \tau_d$. ‖n.a., not applicable. πValues significantly different from IFMQ3, with a probability <0.05 resulting from random variation (based on Student's unpaired *t* test).

neutralization of that charge will remove ~8% of the total gating charge. A decrease of 8% would not be detected by the analysis of conductance–voltage curves. The most definitive approach to determining the role of each charged residue in gating is to examine the effects of the mutations on the gating currents, as has been done for the *Shaker* potassium channel (Perozo et al., 1992, 1994; Sigg and Bezanilla, 1997). These studies are in progress.

Of the mutations that shifted the $v_{1/2}$ for activation, the most pronounced effects were observed when the fourth charge in each of domains I, II, and III was neutralized. It might be expected that neutralization of a single charge in a domain that contains fewer charges would have larger effects. Domain I contains only four positive charges, domains II and III each contain five positive charges, and domain IV has eight positive charges. The mutations in domains I and II shifted the $v_{1/2}$ in the positive direction, indicating that these two mutations stabilized a resting state compared with an activated state of the channel. Consistent with this interpretation, both mutations also resulted in positive shifts in the time constants for activation (τ_m) and deactivation (τ_d). The double mutant combining these two neutralizations resulted in shifts in the $v_{1/2}$ and time constants in the same direction, only larger, indicating that the effects of the two neutralization mutations are at least additive.

On the other hand, neutralization of the fourth charge in domain III (3R4Q) shifted the $v_{1/2}$ for activation in the negative direction, suggesting that an activated state has been stabilized compared with a resting state. The negative shift in τ_d is consistent with this interpretation, but this mutant also exhibited a positive shift in τ_m, which is the opposite of what would be expected. It is clear that this residue in domain III is particularly sensitive to the structure of the amino acid, because the charge-conserving mutation (3R4K) demonstrated large positive shifts in $v_{1/2}$ and τ_d, and a small positive shift in τ_m. Therefore, substitutions at this position alter the conformation of the protein either in both resting and activated states, or in a transitional state between the two, accounting for the slowing down of both activation and inactivation. The 3R4Q mutation significantly increased the time constants for activation (τ_0) and deactivation (τ_{-50}), consistent with an increase in the energy barrier for the transition. Neutralization of the charges in domain IV had the smallest effects on activation, with only a minor shift in $v_{1/2}$ for 4R2Q and no shift for 4R4Q.

Most of the mutations that affected the kinetics of activation and deactivation had comparable effects on the two time constants, with the notable exception of 3R4Q as described above. However, it is not possible to compare the absolute values of the time constants for activation (τ_m) and deactivation (τ_d) because there is essentially no overlap in the voltage regions for which the two were determined. The time constants for activation (τ_m) were determined at potentials equal to or more positive than −30 mV (Fig. 5). In contrast, the time constants for deactivation (τ_d) for most of the mutants were determined at potentials equal to or more negative than −40 mV (Fig. 7). The maximum values for τ_m were ~10 ms at −30 mV, and the maximum values for τ_d were ~2 ms at −40 mV. Because these voltages were in the regions in which each time constant was most rapidly increasing, we do not know if this apparent difference represents a real feature of the channel kinetics.

Two previous studies have also examined the effects of mutations that neutralize the S4 charges in the sodium channel. Stühmer et al. (1989) studied the effects of mutations in domains I and II in the rat brain II channel using macropatch recording of *Xenopus* oocytes. Chen et al. (1996) investigated the effects of mutations of the first and third charges in all four domains of the human heart 1 channel using two-electrode voltage clamping of oocytes. All three studies used different electrophysiological recording techniques, and Chen et al. (1996) examined a completely different channel (the rat brain II and IIA channels are identical in the four S4 regions). In addition, both of the previous studies examined sodium channels with fast inactivation intact, whereas our experiments were carried out with fast inactivation removed. Despite these differences, the results for the wild-type channel are remarkably similar in all three cases. For the voltage dependence of activation, Stühmer et al. (1989) obtained $v_{1/2}$ of -32.7 ± 7 mV, Chen et al. (1996) obtained $v_{1/2}$ of -31.9 ± 0.79 mV, and we obtained $v_{1/2}$ of -29.1 ± 2.7 mV. With respect to gating valence, Stühmer et al. (1989) based their analysis on three identical gating charges, so their values should be equivalent to 1/3 of the other two. Multiplying the values from Stühmer et al. (1989) by three, they obtained z_m of 6.3 ± 0.6 e_0, Chen et al. (1996) obtained z_m of 5.6 ± 0.4 e_0, and we obtained z_m of 5.1 ± 1.1 e_0. It might have been expected that removal of fast inactivation would shift the $v_{1/2}$ of activation in the negative direction (Cota and Armstrong, 1989; Gonoi and Hille, 1987). However, this is not the case in all preparations (Nonner et al., 1980; Oxford, 1981; Stimers et al., 1985; Wang and Strichartz, 1985; Wang et al., 1985), and it was not previously observed for either the rat brain II (Stühmer et al., 1989) or IIA (Patton and Goldin, 1991) channel.

The results of the three studies are summarized in Table IV. In domain I, there appears to be a trend such that charges closer to the cytoplasmic side have more effect on the gating process. Neutralization of the charge at position 3 or 4 resulted in a significant depo-

TABLE IV

Summary of Charge-neutralizing Mutation Effects on Activation

Mutant	$v_{1/2}$ shift*	z_m change (e_0)*
	mV	
1R1Q‡	+3.3	−0.6
1R1Q§	−2.0	0.0
1R2Q	−1.0	+0.4
1R2Q§	−8.0	−1.8‖
1R3Q‡	+4.7π	−1.7π
1R3Q§	+12.0	−1.5‖
1K4Q	+18.5π	−1.2π
1K4Q§	+19.0	−0.9‖
2R1Q‡	+13.3π	−1.2π
2R2Q	+4.4π	−1.1π
2R3Q‡	+0.4π	−1.6π
2K4Q	+14.9π	−0.7
2K5Q§	+10.0	0.0
3K1Q‡	−10.4π	−0.5
3R2Q	−0.3	+0.4
3R3Q‡	+5.9π	−2.1π
3R4Q	−18.1π	+0.3
4R1Q‡	+2.3	−1.6π
4R2Q	+3.6π	−0.5
4R3Q‡	+8.6π	−1.6π
4R4Q	+0.4	+0.9

*$v_{1/2}$ and z_m are the half-maximal voltage and gating valence of activation. Data from Stühmer et al. (1989) did not include an assessment of statistical significance. ‡Data from Chen et al. (1996). §Data from Stühmer et al. (1989). ‖The values for z_m from Stühmer et al. (1989) were multiplied by three for comparison because those values were based on three identical gating charges (m^3). πValues statistically significant, with a probability <0.05 resulting from random variation.

larizing shift in $v_{1/2}$ and a significant decrease in z_m, whereas neutralization of the charge at position 1 or 2 did not have a significant effect on either parameter. In contrast, neutralization of each of the charges in domain II significantly shifted $v_{1/2}$ in the positive direction, and neutralization of each of the first three charges significantly decreased z_m. All of the mutations in domains I and II that had significant effects on $v_{1/2}$ shifted it in the positive direction. On the other hand, neutralization of either charge 1 or 4 in domain III shifted $v_{1/2}$ in the negative direction, indicating that the presence of either of these charges stabilize a resting state. Only the neutralization of charge 3 in domain III reduced z_m. Neutralization of charges 2 or 3 in domain IV shifted $v_{1/2}$ in the positive direction, and neutralization of charge 1 or 3 reduced z_m. These results suggest that there is a fundamental difference in the roles of each of the four domains with respect to activation gating, but that all are involved to some extent.

Hodgkin and Huxley (1952) originally proposed that voltage-gated sodium channels contain three activation (m) gates and one inactivation (h) gate. When sodium channels were first cloned, it was tempting to speculate that those gates would correspond to the four S4 regions (Noda et al., 1984). However, it is clear that at least some positive charges in the S4 regions of all four domains are involved in activation as voltage-sensing elements, and that each of the four domains has specialized to some extent. It has previously been suggested that domain IV plays a unique role in coupling activation to inactivation (Chahine et al., 1994; O'Leary et al., 1995; Tang et al., 1996; Chen et al., 1996). The accompanying paper examines the effects of the S4 charge mutations on sodium channel inactivation (Kontis and Goldin, 1997).

We thank Dr. Raymond Smith, Dr. Michael Pugsley, Ted Shih, Marianne Smith, and Dan Allen for helpful discussions during the course of this work, Dan Allen and Ian Jester for help with the experiments, and Mimi Reyes for excellent technical assistance.

This work was supported by grants from the National Institutes of Health (NS-26729) and the National Science Foundation (IBN9221984). A.L. Goldin is an Established Investigator of the American Heart Association.

Original version received 26 February 1997 and accepted version received 23 July 1997.

REFERENCES

Aggarwal, S.K., and R. MacKinnon. 1996. Contribution of the S4 segment to gating charge in the *Shaker* K^+ channel. *Neuron* 16: 1169–1177.

Aldrich, R.W., D.P. Corey, and C.F. Stevens. 1983. A reinterpretation of mammalian sodium channel gating based on single channel recording. *Nature (Lond.).* 306:436–441.

Auld, V.J., A.L. Goldin, D.S. Krafte, W.A. Catterall, H.A. Lester, N. Davidson, and R.J. Dunn. 1990. A neutral amino acid change in segment IIS4 dramatically alters the gating properties of the voltage-dependent sodium channel. *Proc. Natl. Acad. Sci. USA.* 87: 323–327.

Catterall, W.A. 1984. The molecular basis of neuronal excitability. *Science (Wash. DC).* 223:653–661.

Chahine, M., A.L. George, Jr., M. Zhou, S. Ji, W. Sun, R.L. Barchi, and R. Horn. 1994. Sodium channel mutations in paramyotonia congenita uncouple inactivation from activation. *Neuron.* 12:281–294.

Chen, L.-Q., V. Santarelli, R. Horn, and R.G. Kallen. 1996. A unique role for the S4 segment of domain 4 in the inactivation of sodium channels. *J. Gen. Physiol.* 108:549–556.

Cota, G., and C.M. Armstrong. 1989. Sodium channel gating in clonal pituitary cells. The inactivation step is not voltage dependent. *J. Gen. Physiol.* 94:213–232.

Durell, S.R., and H.R. Guy. 1992. Atomic scale structure and func-

tional models of voltage-gated potassium channels. *Biophys. J.* 62: 238–250.

Fleig, A., P.C. Ruben, and M.D. Rayner. 1994. Kinetic mode switch of rat brain IIA Na channels in *Xenopus* oocytes excised macropatches. *Pflugers Arch.* 427:399–405.

Goldin, A.L., T. Snutch, H. Lubbert, A. Dowsett, J. Marshall, V. Auld, W. Downey, L.C. Fritz, H.A. Lester, R. Dunn, W.A. Catterall, and N. Davidson. 1986. Messenger RNA coding for only the α subunit of the rat brain Na channel is sufficient for expression of functional channels in *Xenopus* oocytes. *Proc. Natl. Acad. Sci. USA.* 83:7503–7507.

Gonoi, T., and B. Hille. 1987. Gating of Na channels: inactivation modifiers discriminate among models. *J. Gen. Physiol.* 89:253–274.

Guy, H.R., and P. Seetharamulu. 1986. Molecular model of the action potential sodium channel. *Proc. Natl. Acad. Sci. USA.* 83:508–512.

Hirschberg, B., A. Rovner, M. Lieberman, and J. Patlak. 1995. Transfer of twelve charges is needed to open skeletal muscle Na^+ channels. *J. Gen. Physiol.* 106:1053–1068.

Hodgkin, A.L., and A.F. Huxley. 1952. A quantitative description of membrane current and its application to conduction and excitation in nerve. *J. Physiol. (Cambr.).* 117:500–544.

Jan, L.Y., and Y.-N. Jan. 1989. Voltage-sensitive ion channels. *Cell.* 56:13–25.

Kontis, K.J., and A.L. Goldin. 1993. Site-directed mutagenesis of the putative pore region of the rat IIA sodium channel. *Mol. Pharmacol.* 43:635–644.

Kontis, K.J., and A.L. Goldin. 1997. Sodium channel inactivation is altered by substitution of voltage sensor positive charges. *J. Gen. Physiol.* 110:403–413.

Larsson, H.P., O.S. Baker, D.S. Dhillon, and E.Y. Isacoff. 1996. Transmembrane movement of the *Shaker* K^+ channel S4. *Neuron.* 16:387–397.

Liman, E.R., P. Hess, F. Weaver, and G. Koren. 1991. Voltage-sensing residues in the S4 region of a mammalian K^+ channel. *Nature.* 353:752–756.

Logothetis, D.E., S. Movahedi, C. Satler, K. Lindpaintner, and B. Nadal-Ginard. 1992. Incremental reductions of positive charge within the S4 region of a voltage-gated K^+ channel result in corresponding decreases in gating charge. *Neuron.* 8:531–540.

Logothetis, D.E., B.F. Kammen, K. Lindpaintner, D. Bisbas, and B. Nadal-Ginard. 1993. Gating charge differences between two voltage-gated K^+ channels are due to the specific charge content of their respective S4 regions. *Neuron.* 10:1121–1129.

Lopez, G.A., Y.N. Jan, and L.Y. Jan. 1991. Hydrophobic substitution mutations in the S4 sequence alter voltage-dependent gating in *Shaker* K^+ channels. *Neuron.* 7:327–336.

Mannuzzu, L.M., M.M. Moronne, and E.Y. Isacoff. 1996. Direct physical measure of conformational rearrangement underlying potassium channel gating. *Science (Wash. DC).* 271:213–216.

McCormack, K., L. Lin, and F.J. Sigworth. 1993. Substitution of a hydrophobic residue alters the conformational stability of Shaker K^+ channels during gating and assembly. *Biophys. J.* 65:1740–1748.

Noda, M., S. Shimizu, T. Tanabe, T. Takai, T. Kayano, T. Ikeda, H. Takahashi, H. Nakayama, Y. Kanaoka, N. Minamino, et al. 1984. Primary structure of *Electrophorus electricus* sodium channel deduced from cDNA sequence. *Nature (Lond.).* 312:121–127.

Noda, M., T. Ikeda, H. Suzuki, H. Takeshima, T. Takahashi, M. Kuno, and S. Numa. 1986. Expression of functional sodium channels from cloned cDNA. *Nature (Lond.).* 322:826–828.

Noda, M., and S. Numa. 1987. Structure and function of sodium channel. *J. Receptor Res.* 7:467–497.

Nonner, W., B.C. Spalding, and B. Hille. 1980. Low intracellular pH and chemical agents slow inactivation gating in sodium channels of muscle. *Nature (Lond.).* 284:360–363.

O'Leary, M.E., L.-Q. Chen, R.G. Kallen, and R. Horn. 1995. A molecular link between activation and inactivation of sodium channels. *J. Gen. Physiol.* 106:641–658.

Oxford, G.S. 1981. Some kinetic and steady-state properties of sodium channels after removal of inactivation. *J. Gen. Physiol.* 77:1–22.

Papazian, D.M., L.C. Timpe, Y.N. Jan, and L.Y. Jan. 1991. Alteration of voltage-dependence of *Shaker* potassium channel by mutations in the S4 sequence. *Nature (Lond.).* 349:305–310.

Papazian, D.M., X.M. Shao, S.-A. Seoh, A.F. Mock, Y. Huang, and D.H. Wainstock. 1995. Electrostatic interactions of S4 voltage sensor in Shaker K^+ channel. *Neuron.* 14:1293–1301.

Patton, D.E., L.L. Isom, W.A. Catterall, and A.L. Goldin. 1994. The adult rat brain β_1 subunit modifies activation and inactivation gating of multiple sodium channel α subunits. *J. Biol. Chem.* 269: 17649–17655.

Patton, D.E., and A.L. Goldin. 1991. A voltage-dependent gating transition induces use-dependent block by tetrodotoxin of rat IIA sodium channels expressed in *Xenopus* oocytes. *Neuron.* 7: 637–647.

Perozo, E., D.M. Papazian, E. Stefani, and F. Bezanilla. 1992. Gating currents in *Shaker* K^+ channels. Implications for activation and inactivation models. *Biophys. J.* 62:160–171.

Perozo, E., L. Santacruz-Toloza, E. Stefani, F. Bezanilla, and D.M. Papazian. 1994. S4 mutations alter gating currents of Shaker K channels. *Biophys. J.* 66:345–354.

Schoppa, N.E., K. McCormack, M.A. Tanouye, and F.J. Sigworth. 1992. The size of gating charge in wild-type and mutant *Shaker* potassium channels. *Science (Wash. DC).* 255:1712–1715.

Sigg, D., and F. Bezanilla. 1997. Total charge movement per channel. The relation between gating charge displacement and the voltage sensitivity of activation. *J. Gen. Physiol.* 109:27–39.

Sigworth, F.J. 1995. Charge movement in the sodium channels. *J. Gen. Physiol.* 106:1047–1051.

Stimers, J.R., F. Bezanilla, and R.E. Taylor. 1985. Sodium channel activation in the squid giant axon. Steady state properties. *J. Gen. Physiol.* 85:65–82.

Stühmer, W., F. Conti, H. Suzuki, X. Wang, M. Noda, N. Yahagi, H. Kubo, and S. Numa. 1989. Structural parts involved in activation and inactivation of the sodium channel. *Nature (Lond.).* 339:597–603.

Tang, L., R.G. Kallen, and R. Horn. 1996. Role of an S4-S5 linker in sodium channel inactivation probed by mutagenesis and a peptide blocker. *J. Gen. Physiol.* 108:89–104.

Tytgat, J., K. Nakazawa, A. Gross, and P. Hess. 1993. Pursuing the voltage sensor of a voltage-gated mammalian potassium channel. *J. Biol. Chem.* 268:23777–23779.

Wang, G.K., M.S. Brodwick, and D.C. Eaton. 1985. Removal of sodium channel inactivation in squid axon by the oxidant chloramine-T. *J. Gen. Physiol.* 86:289–302.

Wang, G.K., and G. Strichartz. 1985. Kinetic analysis of the action of *Leiurus* scorpion-toxin on ionic currents in myelizated nerve. *J. Gen. Physiol.* 86:739–762.

West, J.W., D.E. Patton, T. Scheuer, Y. Wang, A.L. Goldin, and W.A. Catterall. 1992. A cluster of hydrophobic amino acid residues required for fast Na^+ channel inactivation. *Proc. Natl. Acad. Sci. USA.* 89:10910–10914.

Yang, N., A.L. George, Jr., and R. Horn. 1996. Molecular basis of charge movement in voltage–gated sodium channels. *Neuron.* 16: 113–122.

Yang, N., and R. Horn. 1995. Evidence for voltage-dependent S4 movement in sodium channels. *Neuron.* 15:213–218.